*Journal of Ceramic Processing Research. Vol. 23, No. 6, pp. 817~822 (2022)*
*(Received 30 March 2022, Received in revised form 2 July 2022, Accepted 23 July 2022)*
*https://doi.org/10.36410/jcpr.2022.23.6.817*

J O U R N A L O F
**Ceramic Processing Research**

# X-ray diffraction and raman spectroscopy studies on calcium modified PZT ($Pb_{(1-x)}Ca_xZr_{0.52}Ti_{0.48}O_3$) ceramics prepared via solid state reaction method and sol-gel technique- a comparative study

**Anupama Sachdeva[a,*], Aarushi[b], Jagneet Kaur Anand[a] and R.P. Tandon[c]**
[a]*Keshav Mahavidyalaya, University of Delhi, Delhi 110034, India*
[b]*Department of Electrical Engineering, Texas A&M University, College Station, Texas 77840, USA*
[c]*Department of Physics and Astrophysics, University of Delhi, Delhi 110007, India*

**$Pb_{(1-x)}Ca_xZr_{0.52}Ti_{0.48}O_3$ bulk ceramic compositions where x=0-0.1 in steps of 0.02 are prepared by solid state reaction method and sol-gel technique. A comparative study on the samples is conducted using XRD and Raman Spectroscopy in order to see the effect of processing conditions. XRD peaks are indexed as per monoclinic phase. In both the series of samples, volume shrinkage of the unit cell is observed in calcium modified samples when compared with unmodified samples. It is interesting to note that the samples derived from solid state reaction exhibit pseudo tetragonal structure while sol-gel derived samples show pseudo rhombohedral structure of their monoclinic unit cell. Similar inference has been made via Raman spectroscopy studies on the studied ceramic compositions prepared via two methods. Raman spectroscopy also reveals the possibility that calcium substitutes for lead.**

**Key words: Sol-gel process, PZT, Perovskite.**

## Introduction

From the family of perovskite ferroelectrics with $ABO_3$ type crystal structure, lead zirconate titanate (PZT) with general formula $PbZr_xTi_{1-x}O_3$ is a solid solution of ferroelectric lead titanate, $PbTiO_3$ and antiferroelectric lead zirconate, $PbZrO_3$. $Pb^{+2}$ ions occupy corners of the perovskite unit cell i.e., A-sites, oxygen, the faces and Zr/Ti ions occupy octahedral voids i.e., B-sites [1, 2]. Different compositions of PZT with different Zr/Ti ratio are reported to have ferroelectric phases: tetragonal phase ($F_T$) in Ti-rich side of the binary system and rhombohedral phase ($F_R$) in Zr- rich side. The boundary line between these two phases called morphotropic phase boundary MPB (where the composition is close to $PbZr_{0.52}Ti_{0.48}O_3$) at which the dielectric and electromechanical properties rise to a great extent has been of great interest to researchers [1-4]. Further, the advancement of various experimental and analytical techniques have kept researchers motivated to still work on PZT compositions near MPB and help improving our understanding on the following issues:

- The exact position of MPB on phase diagram
- Whether this is a coexistence region or a sharp boundary [5-15]
- If it is a coexistence region, the exact reason for its existence i.e., whether compositional fluctuations [6, 7, 9], quenched-in thermal fluctuations [8] or even intrinsic and extrinsic contributions of dielectric and piezoelectric response causing anomalies in these properties near MPB [15].
- Enhancement of piezoelectric response of rhombohedral PZT composition along tetragonal (001) polar direction [16, 17].

Noheda et al. (1999) [18] first threw a new light on MPB of pure PZT system by proposing monoclinic phase, the existence of which could explain the anomalously high piezoelectric response in PZT compositions near MPB. They proposed that instead of a sharp boundary, a third phase i.e., monoclinic phase with lower symmetry lies in between the rhombohedral and tetragonal regions of PZT composition. The polarization vector in this phase, although constrained in the monoclinic plane, is free to rotate within it which makes the phase as one of the rare examples of 2-dimentional ferroelectric phase. This ferroelectric monoclinic phase in $F_M$ (space group $C_m$) serves as a transition bridge between the higher symmetry $F_T$ and $F_R$ phases of PZT system and its direction of polarization can lie anywhere between the (001) polarization direction of the tetragonal phase and the (111) direction of rhombohedral phase. When it is tilted more towards (001), structure of the unit cell is

*Corresponding author:
Tel : +91-11-47083152
Fax: +91-11-47083152
E-mail: anupama_sachdeva@hotmail.com

tetragonal-like or pseudo tetragonal and when it is inclined more towards (111), the unit cell resembles rhombohedral structure or is pseudo rhombohedral. Existence of monoclinic phase near MPB of PZT also improves our understanding on why there is enhancement of electromechanical coefficient along tetragonal (001) direction for a PZT with rhombohedral structure near MPB. Now there have been several reports on the existence of monoclinic phase in MPB region of PZT [19-29]. According to these reports, in this phase, the unit cell is doubled in volume compared to the tetragonal one, with lattice parameters $a_m$ and $b_m$ lying along the tetragonal ($\overline{1}10$) and ($1\overline{1}0$) directions, and $c_m$ tilted slightly away from the (001) direction.

In this paper, we have discussed the results of X-ray diffraction and Raman Spectroscopy studies done on calcium modified PZT ceramics near MPB with different calcium content prepared via solid state reaction method and sol-gel technique. X-ray diffraction peaks of the samples are indexed as per now established monoclinic phase. The values of cell parameters, lattice strain *c/a*, volume of monoclinic unit cell ($V_m$) and volume of equivalent primitive unit cell ($V_P$) are calculated for all the prepared compositions of the two series. The inferences drawn from the Raman spectroscopic studies carried out on the samples at room temperature are presented and are in line with the X-ray diffraction studies. Raman spectroscopy studies also reveal the possibility of calcium replacing lead in $ABO_3$ crystal structure of PZT.

## Experimental

### Synthesis

For preparation of ceramic compositions with titular representations as SGPCZT0, SGPCZT2, SGPCZT4, SGPCZT6, SGPCZT8, and SGPCZT10 corresponding to calcium addition of 0, 2, 4, 6, 8, 10 mol% using sol-gel process (i.e., samples of SGPCZT series), lead acetate trihydrate (>99%, Alfa Aesar) (with 10 mol% extra lead), calcium acetate hydrate (99%, Sigma Aldrich), titanium propoxide (98%, Aldrich) and zirconium propoxide (70 wt% in propanol; 99%, Aldrich) are taken as starting materials for sol preparation. The detailed process for synthesis of sintered bulk ceramics of compositions of SGPCZT series has been described elsewhere [30].

The starting materials for the samples prepared via solid state reaction which are high purity lead (II) oxide (PbO) (< 10 μm, 99.9% by Aldrich), titanium (IV) oxide ($TiO_2$) (99.8% anatase, Aldrich), zirconium (IV) oxide ($ZrO_2$) (< 5 μm, 99% by Aldrich) and calcium carbonate ($CaCO_3$) (99.5% by SISCO Research Laboratories Private Limited) are accurately weighed for preparing the ceramic compositions named for this paper as SSPCZT0, SSPCZT2, SSPCZT4, SSPCZT6, SSPCZT8 and SSPCZT10 corresponding to calcium addition of 0, 2, 4, 6, 8, 10 mol% respectively. The process detail is described in [31].

### Characterization

Bulk density values of the sintered samples of both SGPCZT and SSPCZT series are measured at room temperature by Archemedes' principle. X-ray diffraction (XRD) technique at room temperature using Bruker Model-D8 Discover X-ray powder diffractometer with area detector and using $CuK_\alpha$ radiation ($\lambda$ = 1.5405 Å) has been employed to perform the structural analysis of the sintered samples in a range of Bragg angles 2θ ($20^o \leq 2\theta \leq 70^o$). Raman spectroscopy is performed on the sintered pellets at room temperature using Renishaw inVia Raman Microscope wherein an Ar-ion laser with a wavelength of 514 nm and the output power 100 mW has been used as an exciting source.

## Results and Discussion

### Density measurements

Bulk density values of sintered pellets of SGPCZT and SSPCZT series are given in Table 1. The values are seen to be close to the reported theoretical density value of pure PZT (i.e., ~7.95 g/cm$^3$). However, with calcium substitution, neither a significant change nor a definite trend is observed in the bulk density values of the samples in the studied composition range.

### X-ray diffraction studies

The XRD patterns of sintered pellets of $Pb_{1-x}Ca_x$-$Zr_{0.52}Ti_{0.48}O_3$ with different concentrations of Ca (x = 0, 0.02, 0.04, 0.06, 0.08, 0.10) of SSPCZT series and of SGPCZT series recorded at room temperature are shown in Fig. 1(a) and Fig 1(b) respectively. The XRD patterns of all the samples consist of sharp, distinct single diffraction peaks with pure perovskite phase indicating homogeneity and good crystallization of the samples. Absence of any secondary or pyrochlore phase is suggestive of the complete diffusion of Ca into PZT lattice resulting into a single-phase compound.

It has well been reported in literature that the splitting of the peak at 2θ~44º is ascribed to the

**Table 1.** Bulk density values of the sintered samples of SGPCZT and SSPCZT series measured at room temperature by Archemedes' principle.

| Calcium Conc. (mol %) | Bulk Density (g/cm$^3$) | |
|---|---|---|
| | SSPCZT | SGPCZT |
| 0 | 7.88 | 7.78 |
| 2 | 7.83 | 7.72 |
| 4 | 7.44 | 7.72 |
| 6 | 7.29 | 7.67 |
| 8 | 7.55 | 7.47 |
| 10 | 7.72 | 7.59 |

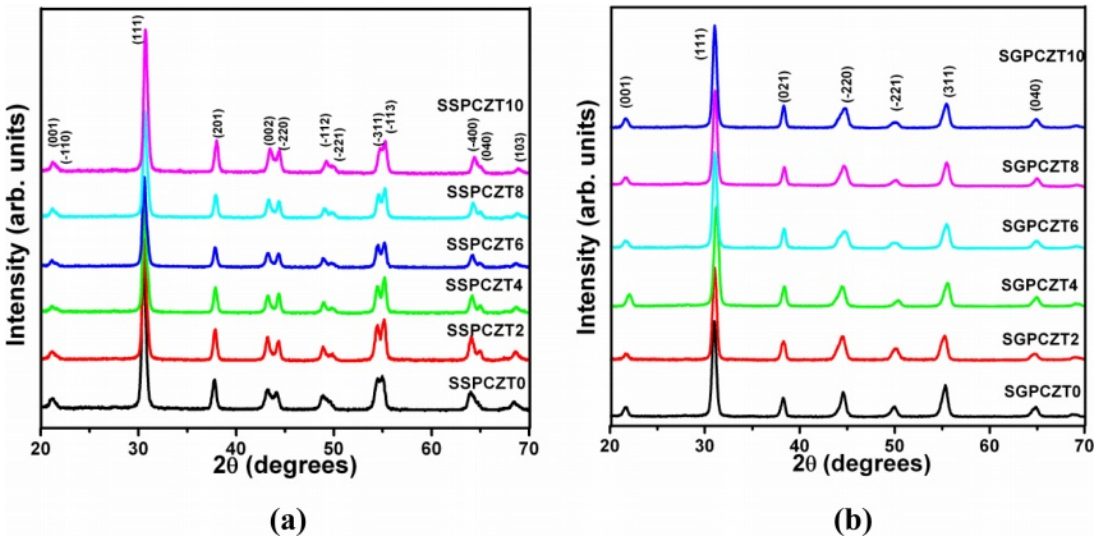


**Fig. 1.** X-Ray Diffraction Patterns of SSPCZT and SGPCZT Series.

tetragonal phase of PZT while that of the peak at 2θ~38º is attributed to the rhombohedral phase [32, 33]. If the two phases coexist as reported in case of the compositions near MPB, a triplet is observed at 2θ~44º [5, 7, 10, 34, 35]. So, apparently, based on these previous reports, the structure for the samples derived here from solid state reaction (SSPCZT series) seems to be tetragonal since the peak at 2θ~44º is well resolved while no splitting is observed for the peak at 2θ~38º in the XRD patterns of SSPCZT series. The XRD patterns of the samples of SGPCZT series here depict that neither the splitting of the peaks at 2θ~44º and 2θ~38º nor a triplet at 2θ~44º are observed but there is anomalous broadening of this peak. The anomalous broadening of the peak at 2θ~44º has been reported to be due to the monoclinic phase of PZT [19] which is now a well established phase for PZT compositions near MPB. Therefore, the indexing of the diffraction peaks was tried using tetragonal, rhombohedral and monoclinic crystal systems using observed interplanar spacing 'd' in a computer program package 'PowderX' [36]. Interestingly, all the patterns of both series could best be fitted as per the monoclinic phase which resulted in the minimum $\Sigma\Delta d = \Sigma(d_{obs}-d_{cal})$. The hkl values, lattice parameters for monoclinic unit cell i.e., $a_m$, $b_m$, $c_m$, $\beta$ and volume $V_m$ were determined corresponding to minimum $\Sigma\Delta d$. The parameters were further refined using CellCalc software [37]. $\beta$ is 90º for a tetragonal cell and it is called the monoclinic angle (≠ 90º) for the monoclinic unit cell. The lattice strain $c/a$ corresponds to $c_t/a_t$, $2\sqrt{2}\ c_m/(a_m+b_m)$ and 1 in the tetragonal, monoclinic and rhombohedral cases respectively [22]. The equivalent elementary perovskite cell parameters of monoclinic phase are given by following equations [22]:

$$a_p=a_m/\sqrt{2} \quad (1)$$

$$b_p=b_m/\sqrt{2} \quad (2)$$

$$c_p=c_m \quad (3)$$

The lattice strain $c/a$ was calculated using the expression:

$$c/a=2\sqrt{2}c_m/(a_m+b_m) \quad (4)$$

Table 2(a) and Table 2(b) provide the values of cell parameters, $c/a$, volume etc. for the calcium modified PZT compositions for SSPCZT and SGPCZT series respectively.

Following observations are also made from XRD studies:

- Volume of the unit cell of the samples prepared via solid state reaction method is greater than that derived from sol-gel method.
- In both the series of samples, volume shrinkage of the unit cell is generally observed with calcium addition when compared with unmodified samples.
- The $c/a$ ratio for all the compositions belonging to SSPCZT series is greater than 1.02 while that of the samples of SGPCZT series is close to 1.

So, while the XRD data could best be fitted according to monoclinic phase, splitting of the peak around although 2θ~44º, no splitting of the peak 2θ~38º and $c/a$ ratio close to 1.02, suggest that the monoclinic unit cell for the compositions of SSPCZT series possess tetragonal-like or pseudo tetragonal structure. And as mentioned above for the samples belonging to SGPCZT series, no splitting of the peak around 2θ~44º, asymmetric broadening of 2θ ~ 38º and $c/a$ ratio near 1 point towards rhombohedral-like or pseudo rhombohedral structure of their monoclinic unit cell.

**Table 2(a).** Values of cell parameters for the calcium modified PZT compositions synthesized by solid state reaction method.

| Sample code | $a_m(Da)$ (Å) | $b_m(Db)$ (Å) | $c_m(Dc)$ (Å) | $\beta(D\beta)$ (deg.) | $V_m(DV)$ (Å$^3$) | $V_p$ (Å$^3$) | $c/a$ |
|---|---|---|---|---|---|---|---|
| SSPCZT0 | 5.81305 (0.00221) | 5.76129 (0.00546) | 4.17514 (0.00350) | 90.222 (0.069) | 139.827 (0.185) | 69.914 | 1.0203 |
| SSPCZT2 | 5.80461 (0.00219) | 5.73605 (0.00258) | 4.17613 (0.00325) | 90.431 (0.059) | 139.043 (0.135) | 69.523 | 1.0235 |
| SSPCZT4 | 5.80053 (0.00169) | 5.73275 (0.00219) | 4.18548 (0.00279) | 90.510 (0.056) | 139.174 (0.114) | 69.589 | 1.0264 |
| SSPCZT6 | 5.79494 (0.00325) | 5.73857 (0.00394) | 4.18434 (0.00505) | 90.384 (0.092) | 139.146 (0.208) | 69.574 | 1.0261 |
| SSPCZT8 | 5.79137 (0.00213) | 5.73353 (0.00277) | 4.17745 (0.00352) | 90.447 (0.071) | 138.708 (0.144) | 69.356 | 1.0252 |
| SSPCZT10 | 5.78113 (0.00163) | 5.72964 (0.00365) | 4.15901 (0.00253) | 90.334 (0.050) | 137.760 (0.127) | 68.881 | 1.0219 |

**Table 2(b).** Values of cell parameters for the calcium modified PZT compositions synthesized by sol-gel method.

| Sample code | $a_m(Da)$ (Å) | $b_m(Db)$ (Å) | $c_m(Dc)$ (Å) | $\beta(D\beta)$ (deg.) | $V_m(DV)$ (Å$^3$) | $V_p$ (Å$^3$) | $c/a$ |
|---|---|---|---|---|---|---|---|
| SGPCZT0 | 5.75446 (0.00126) | 5.74515 (0.00130) | 4.09643 (0.00086) | 90.346 (0.044) | 135.426 (0.051) | 67.714 | 1.0075 |
| SGPCZT2 | 5.75754 (0.00212) | 5.75348 (0.00370) | 4.09949 (0.00148) | 90.334 (0.049) | 135.797 (0.112) | 67.900 | 1.0073 |
| SGPCZT4 | 5.74046 (0.00228) | 5.69576 (0.00603) | 4.07512 (0.00288) | 90.429 (0.035) | 133.238 (0.178) | 66.621 | 1.0079 |
| SGPCZT6 | 5.75506 (0.00206) | 5.71464 (0.00289) | 4.09182 (0.00096) | 90.366 (0.031) | 134.570 (0.089) | 67.286 | 1.0090 |
| SGPCZT8 | 5.74349 (0.00223) | 5.70647 (0.00381) | 4.09266 (0.00145) | 90.368 (0.031) | 134.135 (0.114) | 67.069 | 1.0110 |
| SGPCZT10 | 5.73884 (0.00179) | 5.72681 (0.00696) | 4.09826 (0.00724) | 90.340 (0.053) | 134.688 (0.292) | 67.345 | 1.0110 |

## Raman Spectra Analysis

The Raman spectra recorded at room temperature of SSPCZT and SGPCZT series are depicted in Fig. 2(a) and Fig. 2(b) respectively.

The spectra in general can be divided into frequency regions viz. low frequency (below 150 cm$^{-1}$), mid-frequency (between 150 and 400 cm$^{-1}$) and high-frequency region (above 400 cm$^{-1}$). The spectral region below 150 cm$^{-1}$ contains the external modes of the material. For PZT system, it is related to Pb-lattice modes. The region above 150 cm$^{-1}$ contains internal modes related to bending, torsion and stretching of (Zr/Ti)$O_6$ units [38]. It has earlier been reported [38-40] that sharper peaks in low frequency (~135 cm$^{-1}$) region exhibit the presence of tetragonal phase in PZT while absence of soft modes (i.e., low-frequency modes) is a characteristic of rhombohedral structure. It is also mentioned in these reports that a shoulder around 320 cm$^{-1}$ and splitting of peak around 550 cm$^{-1}$ signify tetragonalilty. But, the absence of shoulder and a broad peak with no splitting around 550 cm$^{-1}$ are signatures of rhombohedral structure. It can also be inferred from the report of Filho et al. [38] that there is an increase in the intensity of $A_1$(1LO) mode as compared to that of E(2TO) with the increase of tetragonality.

Following are some notable features of the Raman spectra recorded at room temperature of the samples of the two series:

- SSPCZT Series:

(a) Presence of sharper peaks in low wavenumber region ~ 135 cm$^{-1}$
(b) Presence of shoulder ~320 cm$^{-1}$ which becomes more prominent with increasing *c/a* ratio
(c) Increased intensity of $A_1$(1LO) mode relative to E(2TO)
(d) No clear splitting of the peak around 550 cm$^{-1}$ in the samples of SSPCZT series. Rather, the peak around 550 cm$^{-1}$ is a broad, diffused peak

Similar observations have been reported for PZT compositions near MPB [39-43].

Although (a), (b), (c) point towards tetragonal structure of the samples of this series but had the structure of the samples be purely tetragonal, clear splitting of the peak around 550 cm$^{-1}$ would also be observed. This suggests that the structure of the samples is not truly tetragonal but tetragonal-like. This

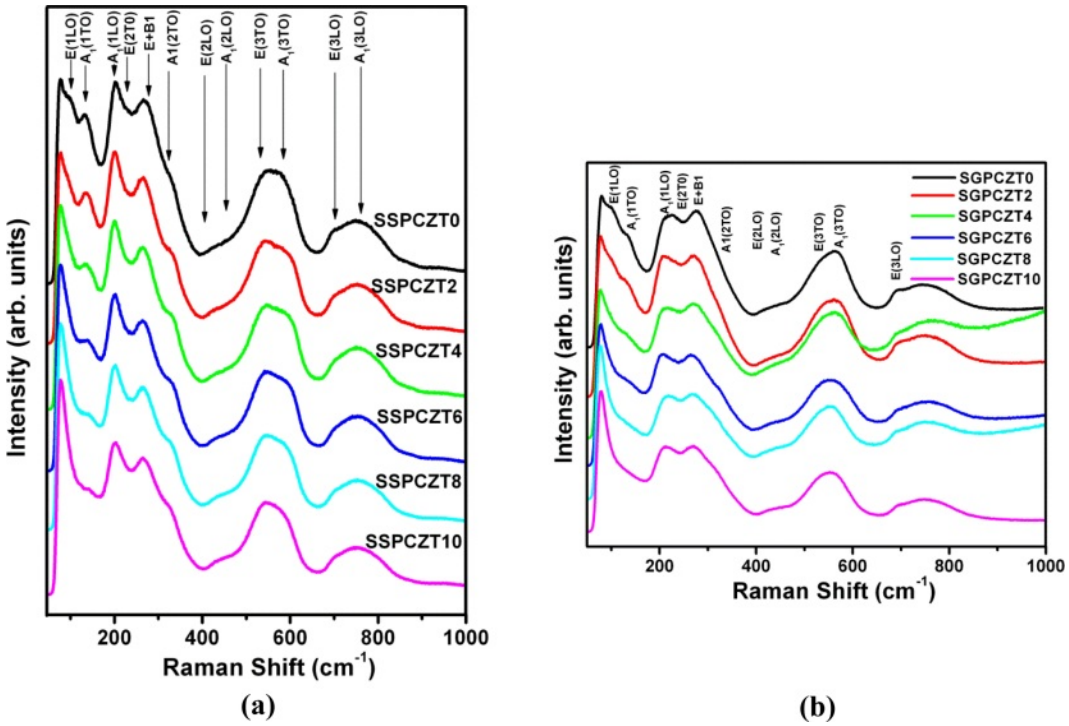


**Fig. 2.** Raman Spectra of SSPCZT Series and SGPCZT.

is well complemented by the inference drawn from the XRD studies.

- SGPCZT Series:

- Presence of broad peaks in low frequency region ~ 135 $cm^{-1}$
- Absence of shoulder around 320 $cm^{-1}$ for the compositions SGPCZT0 and SGPCZT2 and its slight appearance for the remaining compositions of SGPCZT series
- Almost same intensity of A1(1LO) mode relative to E(2TO)
- No splitting of the peak around 550 $cm^{-1}$

all indicate that the structure of the unit cell of the samples of SGPCZT series is rhombohederal-like.

Further, according to previous published reports, $A_1$(1TO) mode shifts towards higher frequency/ wavenumber side if the cation having smaller mass and smaller ionic radius substitutes at A-site. Broadening of the lineshape of this mode has been attributed to the presence of thermodynamically stable defects [41, 42]. So, shifting of the $A_1$(1TO) peak towards higher frequencies and broadening of its lineshape with increasing calcium content for SSPCZT and SGPCZT series as shown in Fig. 3(a) and Fig. 3(b) reflect the possibility of calcium (having smaller mass and smaller ionic radius than lead) substituting for lead at A-site of perovskite structure.

So, the above comparative study gives some insight

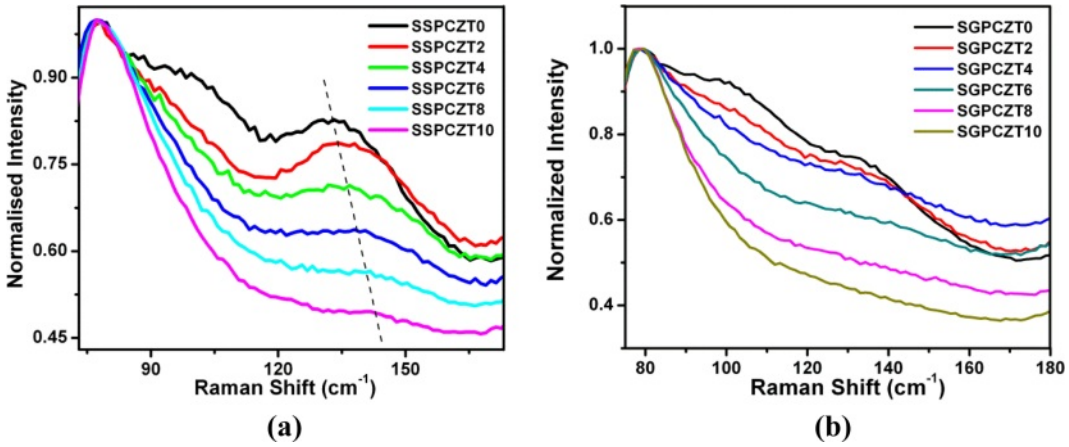


**Fig. 3.** Raman Spectra of SSPCZT and SGPCZT series showing shifting of $A_1$(1TO) peak shift towards higher frequency.

about the effect of processing conditions that can help preparing different strains/structures of the same composition of PZT near MPB.

## Conclusions

- Using different processing conditions, $Pb_{(1-x)}Ca_x$-$Zr_{0.52}Ti_{0.48}O_3$ ceramic compositions with different calcium concentrations have been synthesized having different strains (i.e., pseudo rhombohedral in sol-gel derived ceramics with *c/a* ratio close to 1 and pseudo tetragonal in solid state reaction derived ceramics having *c/a* ratio greater than 1.02) of monoclinic phase.
- Raman studies performed on the samples also indicate the possibility of calcium substitution for lead.

## Acknowledgments

One of the authors (Anupama Sachdeva) is thankful to Dr. Vandna Luthra for her guidance during the course of experimental work.

This research did not receive any specific grant from funding agencies in the public, commercial, or not-for-profit sectors.

## References

1. B. Jaffe, W.R. Cook, and H. Jaffe, in "Piezoelectric Ceramics" (Academic Press, 1971).
2. Y. Xu, in "Ferroelectric Materials and Their Applications" (Elsevier Science, 2013).
3. N.F.K. Bahanurddin, M.H. Jumali, J.J. Mohamed, and Z.A. Ahmad, J. Ceram. Process. Res. 16[2] (2015) 258-261.
4. S.K. Sinha, A.K. Sinha, P. Kour, and P.K. Barhai, J. Ceram. Process. Res. 12[1] (2011) 93-95.
5. A. Ari-gur and L. Benguigui, Solid State Commun. 15[6] (1974) 1077-1079.
6. K. Kakegawa, J. Mohri, K. Takahasi, H. Yamamura, and S. Shirasaki, Solid State Commun. 24[11] (1977) 769-772.
7. K. Kakegawa, J. Mohri, S. Shirasaki, and K. Takahasi, J. Am. Ceram. Soc. 65[10] (1982) 515-519.
8. W. Cao and L.E. Cross, Phys. Rev. B. 47[9] (1993) 4825-4830.
9. A.P. Singh, S.K. Mishra, R. Lal, and D. Pandey, Ferroelectrics. 163[1] (1995) 103-113.
10. K. Kakegawa, O. Matsunaga, T. Kato, and Y. Sasaki, J. Am. Ceram. Soc. 78[4] (1995) 1071-1075.
11. J.C. Fernandes, D.A. Hall, M.R. Cockburn, and G.N. Greaves, Nucl. Instrum. Methods Phys. Res. B. 97[1-4] (1995) 137-141.
12. S.K. Mishra, A.P. Singh, and D. Pandey, Appl. Phys. Lett. 69[12] (1996) 1707-1709.
13. E.R. Leite, M. Cequeira, L.A. Perzaoli, R.S. Nasar, E. Longo, and J.A. Varela, J. Am. Ceram. Soc. 79[6] (1996) 1563-1568.
14. Ragini, R. Ranjan, S.K. Mishra, and D. Pandey, J. Appl. Phys. 92[6] (2002) 3266-3274.
15. Y. Ishibashi, and M. Iwata, Jpn. J. Appl. Phys. 37[8B] (1998) L985-L987.
16. X. Du, J. Zheng, U. Belegundu, and K. Uchino, Appl. Phys. Lett. 72[19] (1998) 2421-2423.
17. B. Noheda, Curr. Opin. Solid State Mater. Sci. 6[1] (2002) 27-34.
18. B. Noheda, D.E. Cox, G. Shirane, J.A. Gonzalo, L.E. Cross, and S.-E. Park, Appl. Phys. Lett. 74[14] (1999) 2059.
19. B. Noheda, J.A. Gonzalo, R. Guo, S.-E. Park, L.E. Cross, D.E. Cox, and G. Shirane, Phys. Rev. B. 61[13] (2000) 8687-8695.
20. L. Bellaiche, A. Garcia, and D. Vanderbilt, Phys. Rev. Lett. 84[23] (2000) 5427-5430.
21. D. Vanderbilt, and M.H. Cohen Phys. Rev. B. 63[9] (2001) 094108(1-9).
22. B. Noheda, D.E. Cox, G. Shirane, R. Guo, B. Jones, and L.E. Cross, Phys. Rev. B. 63[1] (2000) 014103(1-9).
23. K.C.V. Lima, A.G. Souza Filho, A.P. Ayala, J. Mendes Filho, P.T.C. Freire, F.E.A. Melo, E.B. Araújo, and J.A. Eiras, Phys. Rev. B. 63[18] (2001) 184105 (1-5).
24. A.K. Singh, D. Pandey, S. Yoon, S. Baik, and N. Shin, Appl. Phys. Lett. 91[19] (2007) 192904(1-3).
25. X.Q. Ke, D. Wang, X. Ren, and Y. Wang, Phys. Rev. B. 88[21] (2013) 214105(1-6).
26. R.S. Solanki, S.K. Mishra, A. Senyshyn, S. Yoon, S. Baik, N. Shin, and D. Pandey, Appl. Phys. Lett. 102[5] (2013) 052903(1-5).
27. F. Cordero, Materials 8[12] (2015) 8195-8245.
28. L. Fan, J. Chen, Y. Ren, Z. Pan, L. Zhang, and X. Xing, Phys. Rev. Lett. 116[2] (2016) 027601(1-5).
29. J. Zhao, S.D. Funni, E.R. Molina, E.C. Dickey, and J.L. Jones, J. Euro. Ceram. Soc. 41[6] (2021) 3357-3362.
30. A. Sachdeva, V. Luthra, P. Gautam, and R.P. Tandon, Integr. Ferroelectr. 122[1] (2010) 74-82.
31. A. Sachdeva, Aarushi, J.K. Anand, and R.P. Tandon, J. Ceram. Process. Res. 23[1] (2022) 99-108.
32. A. Beitollahi, J. Mater. Sci. 38[6] (2003) 1219-1229.
33. H. Huang, Z. Tianshu, J.T. Oh, and P. Hing, Ferroelectrics. 274[1] (2002) 55-65.
34. A. Boutarfaia, C. Boudaren, A. Mousser, and S.E. Bouaoud, Ceram. Int. 21[6] (1995) 391-394.
35. H. Chen, J. Long, and Z. Meng, Mater. Sci. Eng. B. 99[1-3] (2003) 433-436.
36. C. Dong, J. Appl. Cryst. 32[4] (1999) 838-838.
37. H. Miura, J. Crystallogr. Soc. Jpn. 45[2] (2003) 145-147.
38. A.G. Souza Filho, K.C.V. Lima, A.P. Ayala, I. Guedes, P.T.C. Freire, F.E.A. Melo, J. Mendes Filho, E.B. Araújo, and J.A. Eiras, Phys. Rev. B. 66[13] (2002) 132107(1-4).
39. H. Zhang, S. Leppävuori, and P. Karjalainen, J. Appl. Phys. 77[6] (1995) 2691-2696.
40. J.F. Meng, R.S. Katiyar, G.T. Zou, and X.H. Wang, Phys. Stat. Sol. 164[2] (1997) 851-862.
41. P.S. Dobel and R.S. Katiyar, J. Raman Spectrosc. 33[6] (2002) 405-423.
42. S.R. Shannigrahi and S. Tripathy, Ceram. Int. 33[4] (2007) 595-600.
43. H. Zhang, A. Uusimäki, S. Leppävuori, and P. Karjalainen, J. Appl. Phys. 76[7] (1994) 4294-4300.